

## A damping of the de Haas–van Alphen oscillations in the superconducting state

This article has been downloaded from IOPscience. Please scroll down to see the full text article.

2003 J. Phys.: Condens. Matter 15 239

(<http://iopscience.iop.org/0953-8984/15/2/323>)

View [the table of contents for this issue](#), or go to the [journal homepage](#) for more

Download details:

IP Address: 171.66.16.119

The article was downloaded on 19/05/2010 at 06:28

Please note that [terms and conditions apply](#).

## A damping of the de Haas–van Alphen oscillations in the superconducting state

K P Duncan<sup>1,3</sup> and B L Györfy<sup>2</sup>

<sup>1</sup> Department of Applied Mathematics, The Open University, Milton Keynes MK7 6AA, UK

<sup>2</sup> H H Wills Physics Laboratory, University of Bristol, Tyndall Avenue, Bristol BS8 1TL, UK

E-mail: K.Duncan@open.ac.uk

Received 28 August 2002

Published 20 December 2002

Online at [stacks.iop.org/JPhysCM/15/239](http://stacks.iop.org/JPhysCM/15/239)

### Abstract

Deploying a recently developed semiclassical theory of quasiparticles in the superconducting state we study the de Haas–van Alphen effect. We find that the oscillations have the same frequency as in the normal state but their amplitude is reduced. We find an analytic formula for this damping which is due to tunnelling between semiclassical quasiparticle orbits comprising both particle- and hole-like segments. The quantitative predictions of the theory are consistent with the available data.

The revival of interest [1–3] in studying the de Haas–van Alphen (dHvA) effect in the superconducting state [4] is driven by the hope that this would provide new  $k$ -vector-dependent information about the superconducting gap  $\Delta(k)$ . Evidently this would be of particular importance in connection with anisotropic superconductors where  $\Delta(k)$  can have lines of zeroes on the Fermi surface [5]. Unfortunately at this stage there is no consensus concerning the mechanism of how the experimentally observed oscillations of the diamagnetic response of a type II superconductor come about [6–17] (see [7] for a recent review of the various theoretical approaches). Using our recently developed very general semiclassical theory of quasiparticles in the superconducting state [18], in what follows we develop a semiclassical picture of Landau-like orbits of quasiparticles suggested by the simple model calculation of Miller and Györfy [8]. Clearly the long term aim of a semiclassical theory is to provide an analogue of the Lifshitz–Kosevich (LK) formula for superconductors. Hopefully such a formula would allow the interpretation of experiments in terms of the Fermi surface and the variation of  $\Delta(k)$  on the Fermi surface. At this stage we only deal with conventional superconductors with the usual s-wave pairing. As it happens this is the only case for which reliable data already exists. Within the limits of a number of simplifying assumptions the above semiclassical theory provides for Bohr–Sommerfeld-like quantization rules for quasiparticles.

<sup>3</sup> Previous address: H H Wills Physics Laboratory, University of Bristol, Tyndall Avenue, Bristol BS8, UK.

In particular it allows for the analogue of magnetic breakdown which involves tunnelling between distinct semiclassical orbits. We show that there are orbits which enclose areas that are precisely the same size as the Landau orbits in the normal state, but involve such tunnelling. As will be seen the consequence of these tunnelling events is a damping factor in the LK formulae, in agreement with experiments [1–3].

The theory we wish to use seeks the semiclassical spectrum of the following Bogoliubov–de Gennes (BdG) equations:

$$\begin{pmatrix} \frac{1}{2m}(\hat{\mathbf{p}} + e\mathbf{A}(\mathbf{r}))^2 + V(\mathbf{r}) - \epsilon_F & |\Delta(\mathbf{r})|e^{i\phi(\mathbf{r})} \\ |\Delta(\mathbf{r})|e^{-i\phi(\mathbf{r})} & -\frac{1}{2m}(\hat{\mathbf{p}} - e\mathbf{A}(\mathbf{r}))^2 - V(\mathbf{r}) + \epsilon_F \end{pmatrix} \begin{pmatrix} u_\lambda(\mathbf{r}) \\ v_\lambda(\mathbf{r}) \end{pmatrix} = E_\lambda \begin{pmatrix} u_\lambda(\mathbf{r}) \\ v_\lambda(\mathbf{r}) \end{pmatrix}, \quad (1)$$

where  $u_\lambda(\mathbf{r})$  and  $v_\lambda(\mathbf{r})$  are the probability amplitudes that an elementary excitation is a quasiparticle and quasihole, respectively,  $\Delta(\mathbf{r}) = |\Delta|e^{i\phi(\mathbf{r})}$  is the order parameter and the other symbols have the conventional meaning. For type II superconductors in large magnetic fields  $\Delta(\mathbf{r})$  takes the form of the Abrikosov flux lattice [19], comprising a periodic array of vortices. The effective classical mechanics, Hamilton–Jacobi equations for the quasiparticles, corresponding to (1), is described by the following effective Hamiltonians [18]:

$$E^\alpha(\mathbf{p}, \mathbf{r}) = \mathbf{p} \cdot \mathbf{v}_s(\mathbf{r}) + \alpha \sqrt{\left(\frac{p^2}{2m} + \frac{1}{2}m\mathbf{v}_s^2(\mathbf{r}) + V(\mathbf{r}) - \epsilon_F\right)^2 + |\Delta(\mathbf{r})|^2}, \quad (2)$$

where  $\alpha = \pm$  and  $m\mathbf{v}_s(\mathbf{r}) = \frac{1}{2}\hbar\nabla\phi(\mathbf{r}) + e\mathbf{A}(\mathbf{r})$  is the superfluid velocity. On a constant energy surface these determine, implicitly, the functions  $\mathbf{p}^\alpha(\mathbf{r})$  to be used in the Bohr–Sommerfeld quantization rule. To simplify matters we take the crystal potential  $V(\mathbf{r})$  to be a constant. It is clear from the single vortex solution [18] that the detailed shape of  $|\Delta(\mathbf{r})|$  is not essential. This fact will be used below. In contrast the role of the line of phase singularities [18], which runs along the vortex core, needs more careful consideration. The topologically non-trivial behaviour of the phase gradient ( $\oint \nabla\phi \cdot d\mathbf{r} \neq 0$  for any path enclosing lines of phase singularities) causes the phase gradient,  $\nabla\phi$ , to cancel out (on the average) the increase in  $\mathbf{A}(\mathbf{r})$  across the cell. Consequently the Abrikosov form for  $\mathbf{v}_s(\mathbf{r})$  is periodic. The Hamiltonian, (2), then describes quasiparticles which correspond to spinor Bloch waves [20]. On the other hand, the topologically non-trivial behaviour of  $\Delta(\mathbf{r})$  arises from the superposition of topologically *trivial* solutions to the Ginzburg–Landau theory, so long as the coefficients are suitably determined from minimization of the free energy for the nonlinear problem [19]. In the light of these observations there are two different approaches that can be taken given the Hamiltonian (2). The first is to study and quantize the dynamics described by (2) with a full periodic  $\Delta(\mathbf{r})$  and full  $\mathbf{v}_s(\mathbf{r})$ . This is a formidable task which is not yet complete. The second approach, presented in this paper, is to start by considering the solution of the BdG equations for a topologically trivial  $\Delta(\mathbf{r})$  of the form

$$\Delta(\mathbf{r}) = |\Delta(y)| \exp(ik_x x), \quad (3)$$

with

$$|\Delta(y)| = \Delta_0 \exp\left[-\frac{1}{2}\left(y - \frac{\hbar k_x}{2eB}\right)^2 / ((2\pi)^{-1}d^2)\right], \quad (4)$$

and  $k_x = 2\pi n/d$  ( $d$  is the flux lattice cell size and  $n$  is an integer). A full Bloch wave solution to equation (1) can then be constructed by forming an appropriate superposition of solutions using (3) and determining the coefficients from self-consistency. (Note the seemingly innocent plane wave in (3) is responsible for creating an interference between terms, resulting

in a topologically *non-trivial* superposition.) Now the single-valuedness of each solution for (3) ensures the resulting superposition is also single-valued. Since the former requires the quantization of a Bohr–Sommerfeld integral for quasiparticles with the  $\Delta(\mathbf{r})$  given above, and quantizing the Bohr–Sommerfeld integral yields the spectrum, a solution using (3) is a shortcut to the spectrum, if not the full  $u_\lambda, v_\lambda$  (which obviously requires further work).

Taking this approach, and working in the Landau gauge, we rewrite (2) as

$$E^\alpha(\mathbf{p}, \mathbf{r}) = P_x v_{s,x}(y) + \alpha \sqrt{\left(\frac{p^2}{2m} + \frac{1}{2} m v_{s,x}^2(y) - \epsilon_F\right)^2 + |\Delta(y)|^2}, \quad (5)$$

where  $m v_{s,x}(y) = \hbar k_x/2 + e A_x(y)$  and we have approximated  $\mathbf{B}(\mathbf{r}) = \nabla \times \mathbf{A}(\mathbf{r})$  by a constant (averaged)  $\mathbf{B}$ -field. The quasiparticle dynamics described by (5) are integrable and we can deploy the full semiclassical machinery developed in [18]. This we now do.

The momentum branches defined by the Hamilton–Jacobi equations  $E^\alpha(\mathbf{p}, \mathbf{r}) = E^\alpha$  are

$$p_y^{\pm,\alpha}(y) = \sqrt{p_F^2 - P_x^2 - p_z^2 - m^2 \omega_c^2 \tilde{y}^2 \pm 2m \sqrt{(E^\alpha + P_x \omega_c \tilde{y})^2 - |\Delta(y)|^2}}, \quad (6)$$

where  $\tilde{y} = y - \hbar k_x/2eB$ . We see immediately that  $\frac{\hbar k_x}{2eB}$  behaves like an orbit centre (shifting the  $y$  coordinate), though restricted to  $\frac{\hbar k_x}{2eB} = nd$  ( $n$  integer). Less obviously,  $P_x$  also behaves like an orbit centre (see below). It is natural to restrict it to one flux cell, i.e.  $-\frac{d}{2} \leq \frac{P_x}{eB} \leq \frac{d}{2}$ . Then, since  $\frac{P_x}{eB}$  lies within a cell, and  $\frac{\hbar k_x}{2eB}$  represents translations by lattice cell vectors, the combined pair allow us to centre orbits anywhere in the sample. As we will see, different placements of orbits within a cell lead to different  $E_\lambda$ , i.e. degeneracy within a cell is lifted. On the other hand, translations of such an orbit by lattice vectors (different choices of  $k_x$ ) leave  $E_\lambda = E_\lambda(P_x)$  invariant. One further simplification replaces  $|\Delta(y)|$  by  $\langle |\Delta(y)| \rangle = |\Delta|$  in the region of interest. Outside this region we expect to set  $|\Delta(y)| = 0$  but, since from (6) any choice in the range  $0 \leq \Delta(y) \leq |\Delta|$  for  $y - \hbar k_x/2eB > d$  makes little difference, we can for simplicity still take  $|\Delta(y)| = |\Delta|$ . Taking all these observations into account the constant energy orbits corresponding to these relations are the same as those studied by Burmistrov and Dubovskii [15]. Firstly we investigate the orbits and spectrum for  $P_x = 0$ . Figure 1(a) shows typical classical phase space orbits defined by (6) with  $P_x = 0$ . The corresponding Bohr–Sommerfeld quantization condition yields

$$E_n^\pm(p_z) = \pm \sqrt{\left(\hbar \omega_c \left(n + \frac{1}{2}\right) + \frac{p_z^2}{2m} - \epsilon_F\right)^2 + |\Delta|^2}. \quad (7)$$

This is the Landau level spectrum, shifted into two square root singularities (figure 2), which was studied previously by Miller and Györfly [8] and Miyake [11]. As it turns out this theory is over-simplified but nevertheless it contains the basic physics. The picture is one of Landau levels which march across the gap [8] giving the same frequency as in the normal state, but with an extra damping, due to  $|\Delta|$  [8, 11], given by  $R^{sc} = a K_1(a)$ , with  $a = 2\pi \ell \frac{|\Delta|}{\hbar \omega_c}$ , ( $\ell$  integer), where  $K_1$  is the Bessel function for imaginary argument. Whilst  $R^{sc}(a)$  fits the experimental data it predicts too much damping for realistic values of  $|\Delta|$ . However, as was pointed out in [15]  $P_x \neq 0$  changes the spectra drastically because, as is clear from (5), ‘Landau level’ energies depend upon  $P_x$ . The rest of this paper deals with these complications.

Thus we consider the orbits and spectrum for  $P_x \neq 0$ . Figures 1(b)–(d) demonstrate the marked change in the structure of the phase space orbits as  $P_x$  increases from zero (figure 1(a)). To understand the behaviour of the branches of  $p_y^{\pm,\alpha}$ , it is helpful to view the orbit structure as resulting from the competition between two different types of turning point. The usual turning points,  $p_y^{\pm,\alpha} = 0$ , are due to the harmonic oscillator confining potential,  $\frac{1}{2} m \omega_c^2 \tilde{y}^2$  ( $\tilde{y} = y - \hbar k_x/2eB$ ) in (6) and are those seen in figures 1(a) and (b). However, the presence

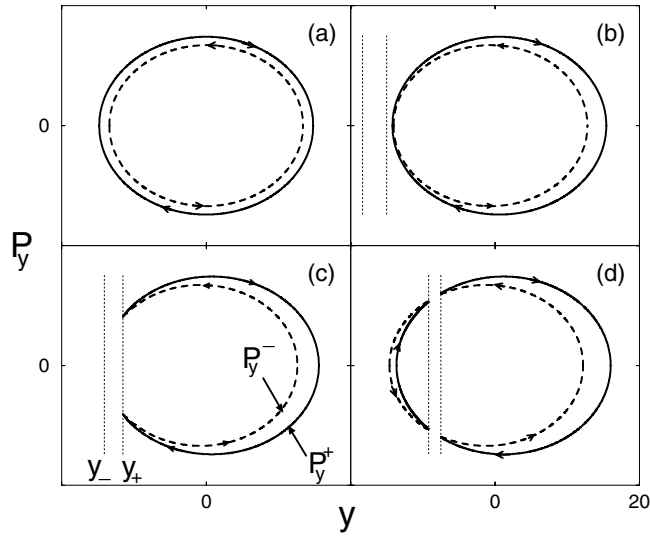


**Figure 1.** Phase space orbits defined by  $p_y^{\pm,\alpha}$  given in (6) with  $|\Delta(y)| = |\Delta|$ . The full curve is for a particle-like excitation, the broken curve is for a hole-like one. Arrows indicate the direction of the velocity. (a)  $P_x = 0$ . The turning points along the  $y$  axis are given by  $p_y^{\pm,\alpha} = 0$ . (b)  $P_x \neq 0$  and small. The orbits are shifted in opposite directions. The vertical dotted lines indicate the position of the Andreev-like turning points,  $y_+(P_x)$  and  $y_-(P_x)$ , see equation (8). (c) As  $P_x$  increases further the Andreev-like turning point  $y_+$ , for which  $p_y^{\pm,\alpha} \neq 0$ , is reached before the normal turning points given by  $p_y^{\pm,\alpha} = 0$ . MAS takes place (see text). (d)  $P_x$  increases even further. Now MAS also occurs at  $y_-$  creating a second particle-hole orbit. The two orbits are separated in real space by  $\delta y = 2|\Delta|/P_x \omega_c$ .

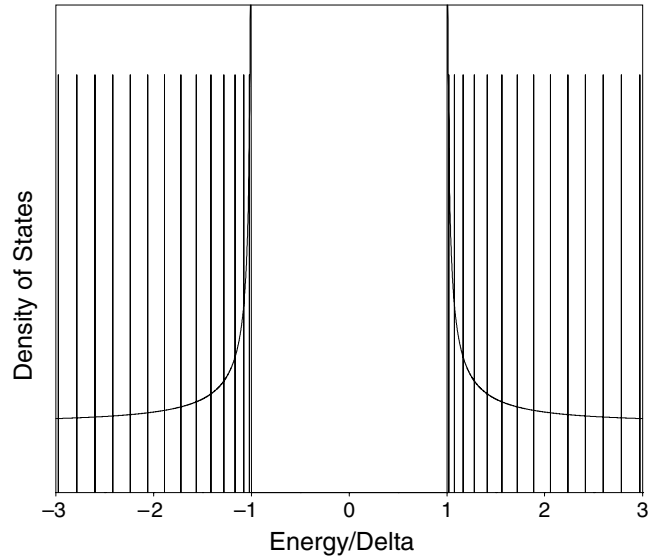


**Figure 2.** Landau level spectrum defined by (7). The BCS density of states is included to emphasize how it is broken in a magnetic field into Landau levels, which are nonetheless pushed apart by the gap,  $|\Delta|$ .

of the second square root in (6),  $\sqrt{(E + P_x \omega_c \tilde{y})^2 - |\Delta|^2}$ , which we denote by  $\epsilon(\tilde{y})$  provides an alternative reflection mechanism for which  $p_y^{\pm, \alpha} \neq 0$ . If  $\epsilon(\tilde{y})$  becomes zero before the normal turning points are reached the momentum becomes complex and the wavefunction will correspondingly exhibit evanescent decay. Classically the excitation undergoes reflection. These new turning points given by  $\epsilon(\tilde{y}) = 0$  are

$$y_{\pm} = \frac{\pm |\Delta| - E}{P_x \omega_c}. \quad (8)$$

This reflection process is analogous to Andreev scattering [21]. Andreev scattering is due to scattering from inhomogeneities in  $|\Delta(\mathbf{r})|$ . Thus  $\sqrt{E^2 - |\Delta(\mathbf{r})|^2} \rightarrow 0$  as  $|\Delta(\mathbf{r})| \rightarrow E$  from below. The reflection process we consider has  $|\Delta| = \text{constant}$ , but due to the non-zero vector potential the extra term,  $P_x \omega_c \tilde{y}$ , can still cause  $\epsilon(\tilde{y}) \rightarrow 0$ . (It is for this reason that the detailed shape of  $|\Delta(y)|$  is not essential.) To emphasize the similarity of this process to Andreev reflection and the role of the vector potential we shall call the scattering mechanism magnetic Andreev scattering (MAS) and  $y_{\pm}$  Andreev-like turning points.

The appearance of MAS when  $P_x$  is varied (figures 1(c) and (d)) can then be explained as follows. From (8) we see that, as  $P_x \rightarrow 0$ ,  $y_{\pm} \rightarrow -\infty$  ( $E \geq |\Delta|$ ). When  $P_x$  becomes non-zero the Andreev-like turning points move in from  $-\infty$  towards the normal turning points. We also see, as stated above, that  $P_x$  acts essentially like an orbit centre, the particle- and hole-like orbits (see below) being pulled in *opposite* directions due to their opposite charge (figure 1(b)). The orbits first intersect when  $p_y^+(y_+) = p_y^-(y_+)$ , i.e. when the Andreev-like turning point reaches the normal turning point. For a more physical picture of the nature of these turning points remember that the spinor (the eigenfunction to (1)) being transported along a given trajectory has both particle,  $|u|$ , and hole,  $|v|$ , amplitudes and thus carries an effective charge  $e^* = e(|u(\mathbf{r})|^2 - |v(\mathbf{r})|^2)$ . Evidently  $e^*(\mathbf{r})$  is a function of position and, in particular, changes from  $e^* > 0$  along  $p_y^+$  (figure 1(c)), through zero (at the turning point) to  $e^* < 0$  along  $p_y^-$ . So the effective charge of the excitation changes sign at  $y_+$  and correspondingly the direction of circulation in the magnetic field is reversed. A particle-like excitation is reflected as a hole-like excitation, and a given orbit has both particle- and hole-like segments.

Having discussed the appearance and interpretation of the MAS orbits we now turn to their quantization. The spectrum obtained from semiclassical quantization is shown in figure 3. Firstly, note that at  $P_x = 0$  there are Landau levels corresponding to (7) which are excluded from the gap. As we increase  $P_x$  we reach the situation shown in figure 1(c). The sensitive dependence of the turning point  $y_+(P_x)$  upon  $P_x$  results in a spectrum which is highly  $P_x$  dependent. Increasing  $P_x$  further results in the situation shown in figure 1(d). The dramatic new feature of the spectrum for  $P_x \neq 0$  is the existence of states inside the gap. These states are new features of the theory which were not there in the  $P_x = 0$  case. However, despite the existence of these states it is clear that they cannot account for the experimental facts on their own. These states have considerably different phase space (and hence momentum space) areas, so that the dHvA frequency for each individual orbit, which is related to this area, will be very different from that in the normal state. To explain the experiments we, in fact, require one further bit of physics. This is a phenomenon analogous to ‘magnetic breakdown’, [23, 24] which we shall now discuss.

We observed that the separation of the two orbits in figure 1(d) is given by  $\delta y = y_+ - y_- = 2|\Delta|/P_x \omega_c$  and is thus inversely proportional to both  $P_x$  and the  $\mathbf{B}$  field (through  $\omega_c = eB/m$ ). For a fixed  $B$ , as  $P_x$  increases this separation in real space rapidly shrinks and quasiparticle tunnelling becomes a viable option. Purely on physical grounds we see that tunnelling between orbit segments (figure 4) can reproduce an orbit in phase space with approximately the normal area. To quantize explicitly the tunnelling orbit the Bohr–Sommerfeld integral can be represented as a complex contour integral. The Riemann surface for the problem is somewhat

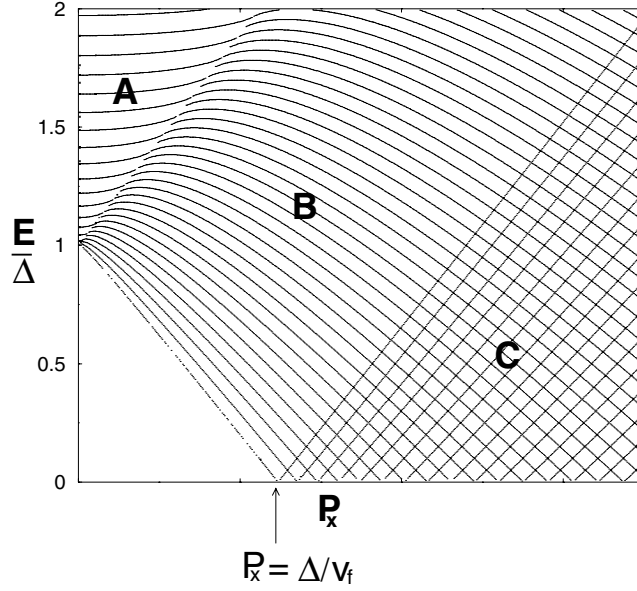


**Figure 3.** Semiclassical spectrum obtained by quantizing the orbits in figure 1. Region A corresponds to quantizing the orbits in figures 1(a) and (b), whilst regions B and C correspond to quantizing the one or two scattering orbits in figures 1(c) and (d). The spectrum first becomes gapless when  $P_x = p_{min} \approx |\Delta(B)|/v_F$ .

similar to that of Fortin *et al* [22]. In our case the MAS orbits live on two different sheets of the Riemann surface but the tunnelling orbit remains on only one sheet. Consequently the integral is equal to the residue at  $\infty$ , on this sheet, and we find

$$E_n(p_z) = \hbar\omega_c \left( n + \frac{1}{2} \right) + \frac{p_z^2}{2m} - \epsilon_F. \quad (9)$$

The spectrum is  $P_x$ -independent and the tunnelling orbits have exactly the normal state frequency. However, the tunnelling coefficient, which depends upon the imaginary part (Im) of the momentum, is

$$T(P_x) = \exp\left(-\frac{1}{\hbar} \left| \int_{y_-(P_x)}^{y_+(P_x)} dy' \text{Im } p_y^\pm(y') \right| \right), \quad (10)$$

and clearly depends upon  $P_x$  and  $B$ . For fixed  $P_x$ ,  $\delta y \propto 1/B \rightarrow 0$  as  $B$  increases, so that the possibility of tunnelling is enhanced. We can therefore view the tunnelling as ‘magnetic breakdown of MAS orbits’. Magnetic breakdown in the normal state is a well studied phenomena [22]. The oscillatory magnetization formula is modified due to the tunnelling. To account for this we must include the factor  $T^{2k}$  (every revolution of the orbit we pick up two tunnelling coefficients, and in general we have  $k$  revolutions). The  $P_x$  dependence of (10) requires the  $\sum_{P_x} T^{2k}$  to be carried out when calculating the magnetization. (An additional  $\sum_{k_x}$  yields the usual degeneracy factor in the formula for the magnetization.) Observing that  $P_{x,max}^2 \ll p_F^2$  we find  $\hbar^{-1} \int dy' \text{Im } p_y^\pm(y') \approx \frac{\pi}{2} \frac{|\Delta|^2}{\hbar\omega_c} \frac{1}{v_F} \frac{1}{P_x}$ , where  $v_F$  is the Fermi velocity. Using  $|\Delta(B)| = \Delta(0)(1 - B/B_{c2})^{1/2} \rightarrow 0$  as  $B \rightarrow B_{c2}$  we have the important observation that  $T(P_x) \rightarrow 1$  for all  $P_x$  as  $B \rightarrow B_{c2}$ . Thus the additional damping vanishes as  $|\Delta| \rightarrow 0$ , as is to be expected. Note that tunnelling is not a small correction: it is zeroth order. The normal state is recovered for  $T(P_x) \rightarrow 1$ .

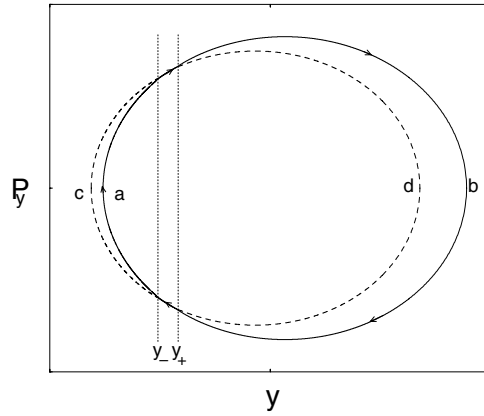


**Figure 4.** The tunnelling orbit (—) comprised of segments from both of the MAS orbits. Tunnelling from  $y_+$  to  $y_-$  results in an orbit with precisely the same phase space area as for an orbit in the normal state. The spectrum quantizing such an orbit is given in equation (9).

The main contribution to  $\sum_{P_x} T^{2k}(P_x)$  is obtained for the largest value of  $P_x = eBd/2$  and is given by

$$T^{2k}(P_x = eBd/2) = \exp\left(-2^{\frac{3}{2}}\pi^{\frac{1}{2}}k\frac{|\Delta|^2}{\hbar\omega_c}\frac{\Lambda}{v_F}\right), \quad (11)$$

where  $\Lambda = (2eB\hbar)^{-1/2}$ . Interestingly this result is very similar to that found by Maki [9] and Stephen [10] (see also Wasserman and Springford [14]). However, in our case (11) is a gross approximation. More generally, we find the extra damping factor in the superconducting state to be

$$R^{sc}(B) = \frac{1}{p_d} \int_{p_{min}(B)}^{p_d(B)} dP_x \exp\left(-\frac{2k}{\hbar} \left| \int_{y_-(P_x, B)}^{y_+(P_x, B)} dy' \operatorname{Im} p_y^\pm(y', P_x) \right| \right), \quad (12)$$

where  $p_d = eBd/2$ , and  $p_{min}(B) \cong |\Delta(B)|/v_F$  is the smallest value of  $P_x$  for which the spectrum is gapless (see figure 3). Although the above results have been derived for a free-electron model with short-range attraction, constant (averaged) pairing potential ( $|\Delta|$ ) and uniform magnetic field  $\mathbf{B}$ , provisionally the formula for the damping factor given in (12) can be compared with that deduced from experiments. We replace  $v_F$  by its orbitally averaged quantity and use  $\langle 1/v_F \rangle = m_b/\sqrt{2\hbar eF}$  with  $m_b = 0.9 m_e$ ,  $F = 1560$  T and  $|\Delta| = 4.4$  meV to compare (12) with the data for  $V_3Si$  in figure 5. Even at this early stage we have a satisfactory fit to the data. Clearly,  $|\Delta|$  in the above analysis is an effective quantity whose value cannot be expected to agree with the zero field  $|\Delta|$  of 2.6 meV (see for example [2]). A more detailed analysis of the existing data as well as a more complete presentation of the theory will be given elsewhere<sup>4</sup>.

To summarize we developed a semiclassical theory in the superconducting state. This theory makes it clear that we must consider new semiclassical orbits involving ‘magnetic breakdown’ of MAS orbits. It is these new orbits which, when quantized, have precisely the normal state frequency. The tunnelling involved gives rise to an extra damping in the superconducting state in agreement with experiments in such classic superconductors as  $V_3Si$ . As we have stated in the introduction the long term aim is to derive an analogue of the LK formula applicable to superconductors. The original LK formula owes its success

<sup>4</sup> In preparation.



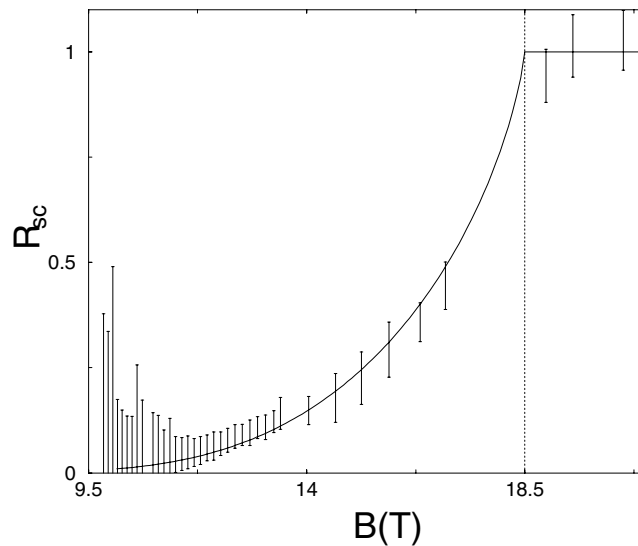


**Figure 5.** Fit of the current theory for the extra damping,  $R^{sc}$ , in the superconducting state to the data for  $V_3Si$  using  $|\Delta| = 4.4$  meV. The upper critical field is  $B_{c2} = 18.5$  T.

to the semiclassical theory of bands in a magnetic field, and it is highly likely that only a semiclassical approach to superconductivity will succeed in incorporating the band structure of these materials. Thus, when generalized to include periodic crystal potential, a more complete description of the flux lattice, and anisotropic pairing [5], the above theory will also be suitable for analysing experimental results on exotic superconductors whenever these become available.

### Acknowledgments

We would like to thank Steve Hayden for supplying us with the data for  $V_3Si$  in figure 5. This work was supported by EPSRC, grant no GR/M53844. The work was carried out at the University of Bristol.

### References

- [1] Onuki Y, Umehara I, Ebihara T, Nagai N and Takita T 1992 *J. Phys. Soc. Japan* **61** 9691
- [2] Janssen T J B, Haworth C, Hayden S M, Meeson P, Springford M and Wasserman A 1998 *Phys. Rev. B* **57** 689
- [3] Goll G, Heinecke M, Jansen A G M, Joss W, Nguyen L, Steep E, Winzer K and Wyder P 1996 *Phys. Rev. B* **53** 8871
- [4] Graebner J E and Robbins M 1976 *Phys. Rev. Lett.* **36** 422
- [5] Mineev V P and Samokhin K V 1999 *Introduction to Unconventional Superconductivity* (London: Gordon and Breach)
- [6] Gor'kov L P and Schrieffer J R 1998 *Phys. Rev. Lett.* **80** 3360
- [7] Maniv T, Zhuravlev V, Vagner I D and Wyder P 2001 *Rev. Mod. Phys.* **73** 867
- [8] Müller P and Györfly B L 1995 *J. Phys.: Condens. Matter* **7** 5579–606
- [9] Maki K 1991 *Phys. Rev. B* **44** 2861–2
- [10] Stephen M J 1992 *Phys. Rev. B* **45** 5481–5
- [11] Miyake K 1993 *Physica B* **186–188** 115–17
- [12] Dukan S and Tešanović Z 1995 *Phys. Rev. Lett.* **74** 2311
- [13] Norman M R, MacDonald A H and Akera H 1995 *Phys. Rev. B* **51** 5927
- [14] Wasserman A and Springford M 1996 *Adv. Phys.* **45** 471

- 
- [15] Burmistrov S N and Dubovskii L B 1996 *Czech. J. Phys.* **46** 895
  - [16] Bruun G M, Nikos Nicopoulos V and Johnson N F 1997 *Phys. Rev. B* **56** 809–25
  - [17] Vavilov M G and Mineev V P 1997 *Sov. Phys.–JETP* **85** 1024
  - [18] Duncan K P and Györfly B L 2002 *Ann. Phys., NY* **298** 273–333
  - [19] Abrikosov A A 1988 *Fundamentals of The Theory of Metals* (Amsterdam: North-Holland)
  - [20] Franz M and Tešanović Z 2000 *Phys. Rev. Lett.* **84** 554
  - [21] Andreev A F 1964 *Sov. Phys.–JETP* **19** 1228
  - [22] Fortin J Y, Bellissard J, Gusmao M and Ziman T 1998 *Phys. Rev. B* **57** 1484
  - [23] Duncan K P 1999 The semiclassical theory of the de Haas–van Alphen oscillations in type-II superconductors  
*PhD Thesis* University of Bristol
  - [24] Duncan K P and Györfly B L 1999 *Bull. APS* **44** 1063